

# STUDY OF POLYMERIC MATERIALS FOR THE FRACTURE OF LARGE BONES.

Juanita Jiménez Montealegre<sup>1</sup>, Uriel Zapata<sup>2</sup>.

**Summary**– This document presents the mechanical evaluation of the design of an implant made of polymeric or composite materials for a fracture in the middle third of the femur through simulations using the Finite Element Method, with which the most suitable material to use is determined based on an existing model of titanium implant; evaluating its physical properties and its behavior in a loading model similar to that which occurs in bone.

**Clinical Relevance** – The use of titanium implants is a very common and appropriate solution for internal fixation between the parts of a broken bone, but in some critical cases their function usually fails due to the stresses generated inside between them, the screws and bone; causing it to fracture again and a new process must be started with a more serious fracture than the one previously treated after a first intervention.

Osteosynthesis fatigue is directly related to the material of which it is composed; this is a damage process that occurs in mechanical elements when they are subjected to variable load states; Regardless of whether these loads are lower with the passage of cycles, their frequency will produce a breakage just like a constant load <sup>[1]</sup>.

Although there are many types of incidents caused after surgery, the possibility of an implant failing due to osteosynthesis fatigue is 22% <sup>[2]</sup>. This may depend on the case to be treated according to the patient and the general care given at the time of beginning a recovery process, or simply due to factors that were present at the time of placing it in the bone.

## I. INTRODUCTION.

Osteosynthesis is a reconstructive surgical process that allows stabilizing and uniting the ends of a broken bone due to a fracture using mechanical elements, allowing partial healing of the bone so that it can recover its joint function <sup>[3]</sup>.

Depending on the severity and type of fracture that may occur in a long bone such as the femur, various methods are usually used to fix it, which involve the use of titanium plates and implants. Although they are usually the most viable solution from a medical point of view, due to the properties that titanium has as a material within medicine and the evolution of these, they can present incidents that harm bone health in the long term by not allowing adequate osteosynthesis and in some cases take the bone to extreme states of loading due to poor placement or extreme cases <sup>[4]</sup>.

Usually, the failure of an implant is due to the fatigue of the osteosynthesis material and the loading cycles to which it is subjected during the time of use; which causes the stability of the system to be lost and the forces to increase until generating

a critical state of load and reaching imminent failure. Furthermore, the shear and bending stresses to which the implant is subjected can cause the material to fatigue and break the bone again, demonstrating that in some cases the implants and screws do not adequately support this type of load.

Considering that these implants are elements for permanent use, in some cases the way in which they retain the bone does not allow it to carry out an adequate osteosynthesis process, which implies that it is not adequately strengthened or 100% functional, limiting the functions that it fulfills in the long term and that it becomes increasingly weaker.

With the aim of simplifying the study of implant behavior, emphasis will be placed on oblique fractures in the middle third of the femur, since this area requires a simpler intervention in relation to the types of implants used and the other areas of the bone. To this end, it is proposed to study, using a polymer or a compound, an alternative that fulfills the same function as titanium implants, and at the same time allows for greater resistance to the loads generated in said area.

## II. MATERIALS AND METHODS.

### A. Design Requirements.

For the development of the prototype, we start from the orthotropic properties of the cortical bone (Table 1) <sup>[20]</sup>, so that they allow us to analyze the behavior of the possible materials in relation to the bone where they are going to be placed.

Cortical Bone Properties			
Property	Units	Minimum Value	Maximum Value
Elastic Limit	MPa	90	144
Density	Kg/m <sup>3</sup>	1800	2080
Fracture Toughness	MPa·m <sup>0.5</sup>	3,5	6,1
Fatigue Resistance at 10 <sup>7</sup> cycles	MPa	23	80
Hardness	HV	50	80
Poisson's ratio	-	0,13	0,3
Shear Rigidity Modulus	GPa	4,5	6,7
Thermal Conductivity	W/m <sup>2</sup> °C	0,41	0,63
Young's Module	GPa	18	26
Specific Heat Capacity	J/Kg°°C	1100	1280

**Table 1.** Orthotropic Properties of Cortical Bone.

These were taken from the **Granta EduPack** software <sup>[5]</sup>, and both mechanical and thermal properties of the bone were observed.

### B. Materials Proposals.

Biomedical materials and their properties were investigated, where the ranges of elastic modulus and thermal conductivity were taken as a reference to search for materials that were like cortical bone.

<sup>1</sup>J. Jiménez is part of the Mechanical Engineering program, Universidad EAFIT, 050022, Medellín, Colombia ([jjimenezm1@eafit.edu.co](mailto:jjimenezm1@eafit.edu.co))

<sup>2</sup>AU. Zapata is with the Faculty of Mechanical Engineering, Universidad EAFIT, 050022, Medellín, Colombia ([uzapata@eafit.edu.co](mailto:uzapata@eafit.edu.co))

The elastic modulus indicates the scale of rigidity of a material, while thermal conductivity allows us to analyze how much capacity a material must conduct heat in relation to the medium where it is located and the elements with which it comes into contact.

From these two properties within *Granta EduPack*, a graph was generated that related the elastic modulus against the thermal conductivity ( $E$  VS  $W/m^{\circ}C$ ), establishing as interval limits the values of (Table 1) <sup>[20]</sup>. The materials that most closely approximate the cortical bone are selected, expanding the graphical search ranges to have more material options for a deeper search.

In this way, the following list of materials was reached, whose properties are shown in (Table 2) <sup>[20]</sup>:

- Poly Ether Ketone with 30% Fiberglass.
- Poly Ether Ether Ketone with 40% Carbon Fiber.
- Polyarylamide with 60% Fiberglass.
- Polycarbonate with 40% Carbon Fiber.
- Modified Poly Ether Ether Ketone with Carbon Fiber between 45% and 55%.

With the materials obtained from (Table 2) <sup>[20]</sup>, a final filter is made, based on the elasticity modulus, where materials with a modulus like that of bone will be considered to evaluate their characteristics within an environment that is already known and apply the charge states in relation to it. This finally leaves us with the following materials from highest to lowest value:

- PARA with 60% Fiberglass.
- PC with 40% Carbon Fiber.
- PEK with 30% Fiberglass.

The properties to perform the simulation with each of these materials are shown in (Table 3) <sup>[20]</sup>, which are required within SolidWorks.

### C. Types of Fixing Plates.

Taking as a key reference the titanium plates for the middle third of the femur and the variety of shapes they have according to their function with the type of fracture (Figure 1) <sup>[20]</sup>, which are listed below along with their characteristics and generalities.

1. **Locked Plates** <sup>[6]</sup>: They allow direct fixation both to the bone and to the plate itself, since they have a thread that coincides with the thread of the screw and limits its movement; thus, achieving stable fixation from compression with the bone.  
Due to the fixation mode, as the axial loading cycles increase, the screws may begin to lose tension, and consequently the friction force decreases, and the implant begins to lose stability until reaching failure <sup>[7]</sup>.
2. **T and Spoon Plates** <sup>[8]</sup>: They are used to relocate the original position of the bone fragments and restore its articular area. Due to the inclination, they must cover the appropriate area, two plates are usually used uniformly on the bone, to avoid the bending effects of overloading one of the ends <sup>[9]</sup>.

3. **Reconstruction Plates** <sup>[10]</sup>: This type of plate allows greater flexibility when placing it in the affected area thanks to the geometry they have, in addition to the fact that they are usually used in areas of greater movement and that do not receive as many consecutive loads <sup>[11]</sup>.
4. **Compression Plates** <sup>[12]</sup>: These compress the ends of a fracture to fix them until reaching a point of stability, thus maintaining the reduction of this and the compression between the parts <sup>[13]</sup>.
5. **Wide Plates** <sup>[8]</sup>: They are designed to withstand large dynamic loads <sup>[14]</sup>, they are usually used in large fragment fractures <sup>[15]</sup> and their placement is defined according to the surgeon's reach. They have 2 variations: Wide Compression and Wide Fine, which meet the same characteristics as a Wide plate, with the difference that the compression plate allows a more direct attachment to the bone due to the geometry and location of the holes.
6. **Narrow Plates** <sup>[8]</sup>: It has the same characteristics of a Wide plate, with the variation that its cross section is smaller and the element or site of placement of the plate is usually more focused <sup>[16]</sup>. It also has 2 variations: Narrow Compression and Narrow Fine, which have the same characteristics as the Wide plates.

### D. 3D Model of the Device.

We will work directly with some existing models of titanium plates for the middle third of the femur, to compare the results between the proposed materials and analyze the viability of adapting them to a new material based on the behavior that they may present. The already existing concepts of titanium plates are shown in (Figure 2) <sup>[20]</sup>.

(Figure 2-a) <sup>[20]</sup> represents a Wide DCP Plate, (Figure 2-b) <sup>[20]</sup> represents a Wide Compression Plate, and (Figure 2-c) <sup>[20]</sup> represents a Narrow-Locked Plate. Each of these models were taken from the *Grab CAD* library <sup>[17]</sup>.

### E. Parameters for Simulation.

#### General Considerations of the Study:

Although there is no single limitation regarding the proposed model due to the variability of cases and fractures, a simple study model was considered that brings together the following:

- Oblique fracture of the middle third of the femur, in which there are large fragments.
- There isn't that big of a gap at the time of break, so there is some stability in the bone.
- The union will be given through stable angle screws or standard screws to allow adequate compression of it to the bone <sup>[18]</sup>.
- The plate should have rounded ends to allow easy insertion without further affecting the bone or the patient <sup>[18]</sup>.

Keeping these considerations in mind, we will work with the model in (Figure 2-a) <sup>[20]</sup>, since it is the one that best adapts to the proposed case study.

### **Loading Conditions:**

Since the model is subjected to the same conditions of the bone, two forces are considered, which refer to the weight of the person and the reaction generated by the contact between the femur and the tibia, which occurs in the knee joint. For this model, an 80 kg person was taken as a reference, whose force in Newtons would be 784.8 N. This will be used in its entirety to evaluate a critical case where the person must stand with only one leg, and the load will be applied at the ends of the plates to simulate the compression that would be generated in the bone.

A lateral force of 0.85 Kg (8.34 N) was also added, which represents a muscular force generated by the vastus lateralis muscle (*Vastus Lateralis*)<sup>[19]</sup>, to correctly simulate the behavior of the implant inside the body.

### **Border Conditions:**

The boundary conditions applied vary according to the type of plate; in the case of the Wide DCP Plate (Figure 3)<sup>[20]</sup>, the holes are fixed symmetrically to simulate the grip of the screw to the bone after being placed and exerting an adequate pressure on the bone.

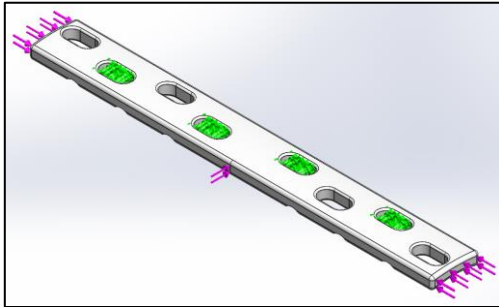


Figure 3. DPC Wide Plate Charging Status.

### **Meshing Parameters:**

To have control over the results and the mesh itself, a custom mesh with small elements was used due to the size of the plates (which are not very large). The mesh type was “Combined Curvature-Based Mesh” due to the variation in plate surfaces and plate geometry.

(Figure 4)<sup>[20]</sup> shows the mesh of the plate to be used for the simulation, as well as an annex of its characteristics in (Table 4)<sup>[20]</sup>.

### **Mesh Convergence Analysis:**

To determine if the behavior of the mesh to be used and its parameters are consistent with the expected results, a convergence analysis was developed based on the three layouts to be studied: Principal stresses, deformations, and unit strains; in the simulation of the PARA at 60% Fiberglass.

For this purpose, different studies were carried out, varying the density of the mesh, and studying the behavior of the results, seeking convergence as the number of elements of each mesh increased until reaching the mesh that was used in the simulation (Figure 4)<sup>[20]</sup>.

## **III. RESULTS.**

This section shows the results of the stresses, strains, and unitary strains, using the three materials that were proposed after their selection. The principal stresses will be given in Mega Pascals (N/mm<sup>2</sup>), the deformations will be given in millimeters (mm) and the unitary strains will be given dimensionless (mm/mm).

### **PARA (60% Fiberglass):**

#### **a) Principal Stress Analysis:**

Considering that composite materials were used as the focus of the work; they cannot be characterized within any category as ductile or brittle. For this case, the compressive stress (P3) was considered, due to the loading state to which it was subjected.

(Figure 5)<sup>[20]</sup> shows the layout that characterizes the wide DCP plate.

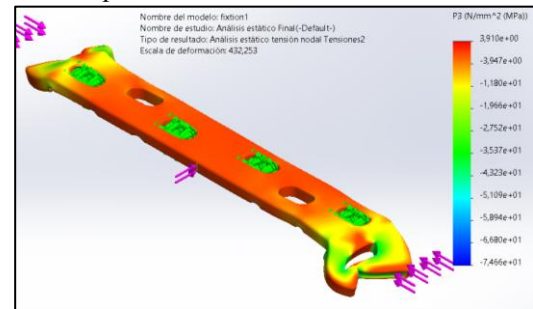


Figure 5. Compressive Stress Wide DPC Plate – PARA.

In the wide DCP plate there is a maximum compressive stress of 3.91 MPa.

#### **b) Deformation Analysis:**

The deformations of the model were determined because of the external forces to which the system is subjected. In the wide DCP plate (Figure 6)<sup>[20]</sup> a maximum deformation of 0.03582 mm occurs at the bottom.

#### **c) Analysis of Unitary Deformations:**

The unitary deformations were studied from the loading state and the model constraints shown in (Figure 3)<sup>[20]</sup>. Static analysis indicates that a maximum strain of 0.002441 occurs in the wide DCP plate (Figure 7)<sup>[20]</sup>.

This same procedure and analysis apply to studies with PEK at 30% Carbon Fiber and PC at 40% Carbon Fiber.

### **PEK (30% Carbon Fiber):**

#### **a) Principal Stress Analysis:**

(Figure 8)<sup>[20]</sup> shows the plot of the simulation results, which indicate that in the wide DCP plate a maximum compressive stress of 4.0 MPa occurred.

#### **b) Deformation Analysis:**

The plot of the deformations is shown in (Figure 9)<sup>[20]</sup>, which gave results of 0.04528 mm for the wide DCP plate.

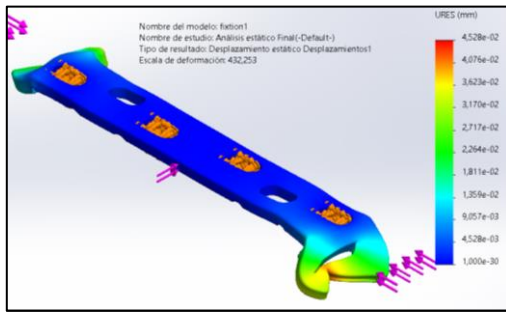


**Figure 9. Wide DPC Plate Deformation - PEK**

**c) Analysis of Unitary Deformations:**

The strain plotting results are shown in (Figure 10) [20], where the wide DCP plate showed a maximum strain of 0.003099.

**PC (40% Carbon Fiber):**

**a) Principal Stress Analysis:**

(Figure 11) [20] shows the plot of the simulation results, which indicate that in the wide DCP plate there was a maximum compressive stress of 3.91 MPa.

**b) Deformation Analysis:**

The plot of the deformations is shown in (Figure 12) [20], which gave results of 0.0398 mm for the wide DCP plate.

**c) Analysis of Unitary Deformations:**

The results of the strain plots are shown in (Figure 13) [20], where the wide DCP plate showed a maximum strain of 0.002712.

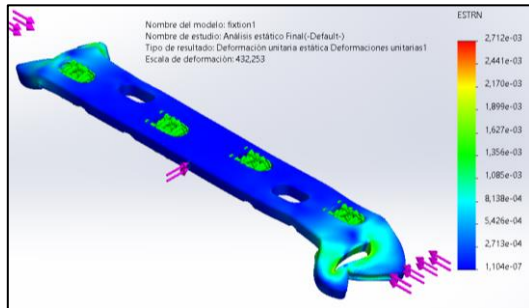


**Figure 13. Unitary Deformation Wide DCP Plate – PC.**

The results of each material study are compiled in (Table 5) [20].

**Convergence Analysis Results:**

A total of eleven variations were made in the density of the model mesh, where each one gave different results as the number of elements increased. This analysis was carried out with the deformations of the model, taking the key points that allowed us to build the graph in (Figure 14) [20].

(Table 6) [20] shows the results and data used for the convergence graph.

**IV. DISCUSSION.**

From this analysis, it was possible to observe and generally understand the behavior of the 3 materials on a model of the device that is already functional, showing the effects of the

forces that acted on it within a realistic model without including the bone. Thanks to this, and to the deformation scales of the system, it was possible to observe a stable model that tends to fail in the middle zone (where the main fastenings are located) due to a compression stress as in (Figures 5, 8 and 11) [20].

The greatest deformations and displacements occurred at the extremes of the model, which was seen at a deformation scale of 432,253 times more exaggerated than the real scale; denoting that the compressive force that was established within the loading conditions can seriously affect the geometry of the implant in the areas of the screw slots (which can be seen at the same time as a stress concentrator).

With the results of (Table 5) [20], it is observed that the three materials used present a very similar behavior between them at the stress level. Regarding deformations, the one that deforms the most is the 30% Carbon Fiber PEK with a displacement of 0.04528 mm, and the one that deforms the least is the 60% Carbon Fiber PARA. The unitary strains showed that the material that deforms the least is the PARA at 60% Fiberglass with unitary strains of 0.002441, and the one that deforms the most is the PEK at 30% Carbon Fiber with unitary strains of 0.003099.

Although the difference between the values expressed is not very high, in loading states with more repeated movement cycles a greater impact may be noted that in the long term may harm the function of the implant, if left inside the body.

It is concluded that all three present similar reactions within the deformation scale of the model and the maximum values shown in (Table 5) [20]. More specifically, it is concluded that the material with the best properties was PARA with 60% Fiberglass, since it is the one that presents the least stress and deformation within the simulation; without leaving aside the fact that PEK with 30% Carbon Fiber and PC with 40% Carbon Fiber can be considered good options for the development of a real prototype of the implant due to their mechanical properties.

Also, it is concluded that it presented adequate behavior and better than that expected for the type of loads to which it was subjected. Although very large and constant load cycles are required for it to deform as shown in (Figures 5 to 13) [20], the model and its restrictions are consistent with the behavior that can occur when evaluating only the plate as an element separated from the bone.

If the model were adapted to a direct evaluation of the implant with the bone, the loading conditions and the behavior of the model would change completely because it would already be a set of parts that would act on their own; so, the reactions that would occur in the implant would be completely different from what was shown previously.

Regarding improvements and observations for the work, it would be considered to develop a simulation of the behavior of the complete bone together with the implant and the screws to understand the effects that may occur in the model when

exposing it to a more realistic situation; and so, observing the effects this can have along with the feasibility of developing a real model.

Within the model studied, more cases can be studied with different types of implants, using the same conditions as in this study and the behavior of the models can be compared to observe the viability of their application.

Finally, the possibility of investigating more material options that resemble or present better properties to the materials shown could be considered; without leaving aside the conditions that were established for its selection in relation to the function that the implant will fulfill in the long term.

## Acknowledgments:

The author thanks to:

- Professor Fanny L. Casado for her contributions when establishing the objectives of this work and the direction during its development.

## V. REFERENCES.

- [1] J. D. Abascal y J. D. Abascal, «La fatiga de los materiales y su tolerancia al da o», *ELMUNDO*, 22 de enero de 2018. [En línea]. Disponible en: <https://www.elmundo.es/economia/2018/01/16/5a5de0e4e5fdeaad3c8b45e5.html>
- [2] N. E. Martínez, «Complicaciones postquirúrgicas y posibles factores de riesgo asociados en pacientes con fracturas diafisarias de fémur o tibia Tratados en el Hospital General de Mexicali de enero de 2018 a enero de 2020», 7 de marzo de 2022. <https://www.medigraphic.com/cgi-bin/new/resumen.cgi?IDARTICULO=103726>
- [3] «Osteosíntesis: qué es, síntomas y tratamiento | Top Doctors», *Top Doctors*, 10 de junio de 2015. <https://www.topdoctors.es/diccionario-medico/osteosintesis>
- [4] R. Orozco, «El ocaso de las placas. ¿Por qué se rompen los implantes?», *Revista Española de Cirugía Ortopédica y Traumatología*, 1 de junio de 2001. <https://www.elsevier.es/es-revista-revista-espanola-cirugia-ortopedica-traumatologia-129-articulo-el-ocaso-placas-por-que-13015919>
- [5] «Ansys Granta EduPack», *Software for Materials Education*, 3 de octubre de 2023. <https://www.ansys.com/products/materials/granta-edupack>
- [6] «Placa 1/3 de tubo bloqueada Titanio – Implantes Center Prot». <http://www.implantescenterprot.com.ar/wp/producto/placa-13-de-tubo-bloqueada-titanio/>
- [7] C. Frías «Placas Bloqueadas», Hospital Veterinario Lepanto. <https://congressohvm.com/1/dw/PlacasBloqueadas.pdf>
- [8] Surgival, «Placas DCP - Placas de osteosíntesis para fracturas | Surgival», *Surgival.com*, 10 de mayo de 2023. <https://www.surgival.com/productos/trauma/placas-dcp/>
- [9] L. A. Zambrano, «Estudio del efecto de placas de fijación en fracturas de tibia proximal utilizando el método de elementos finitos». [http://ve.scielo.org/scielo.php?script=sci\\_arttext&pid=S0376-723X2008000300003#:~:text=La%20t%C3%A9cnica%20de%20osteos%C3%ADntesis%20m%C3%A1s,tornillos%20%5B2%2C3%5D](http://ve.scielo.org/scielo.php?script=sci_arttext&pid=S0376-723X2008000300003#:~:text=La%20t%C3%A9cnica%20de%20osteos%C3%ADntesis%20m%C3%A1s,tornillos%20%5B2%2C3%5D)
- [10] «Placa de reconstrucción bloqueada – Implantes Center Prot». <http://www.implantescenterprot.com.ar/wp/producto/placa-de-reconstruccion-bloqueada/>
- [11] Mario, «Placa de reconstrucción 3.5 – recta», *IMTRA*, 9 de febrero de 2023. <https://imtra.com.mx/producto/placa-de-reconstruccion-35-mm-recta/#:~:text=La%20placa%20de%20reconstrucci%C3%B3n%203.5,tornillos%20de%20esponjosa%204.0%20mm>
- [12] «PLACAS DE COMPRESIÓN BLOQUEADAS – Industrias Medica Sampedro». <https://imsampedro.com.co/blog/portfolio/placas-de-compresion-bloqueadas/>
- [13] C. G. M y D. O. T, «ELEMENTOS DE OSTEOSÍNTESIS DE USO HABITUAL EN FRACTURAS DEL ESQUELETO APENDICULAR: EVALUACION RADIOLOGICA», *Revista Chilena de Radiología*, vol. 11, n.º 2, ene. 2005, doi: 10.4067/s0717-93082005000200005. [https://www.scielo.cl/scielo.php?script=sci\\_arttext&pid=S0717-93082005000200005#figura14](https://www.scielo.cl/scielo.php?script=sci_arttext&pid=S0717-93082005000200005#figura14)
- [14] «PLACA LCP ANCHA DE 4,5 MM». <http://osteosynthesis.com/producto/placa-lcp-ancha-de-45-mm-2/>
- [15] Surgival, «Placa ancha - Surgival», *Surgival*, 27 de julio de 2015. <https://test.surgival.com/portfolio-item/placa-ancha/>
- [16] «Placa FixLOCK estrecha, 4,5 mm | Sistema de placas para grandes fragmentos». <https://es.indianorthopaedic.com/848/placa-fix-em-lock-em-estrecha-4-5-mm.htm>
- [17] «Free CAD designs, files & 3D models | The GrabCAD Community Library». <https://grabcad.com/library>
- [18] MBA, «Sistemas de Osteosíntesis». [https://secot2020.com/wp-content/uploads/2020/10/aap-I.011es-LOQTEQ-PB\\_v10\\_WEB.pdf](https://secot2020.com/wp-content/uploads/2020/10/aap-I.011es-LOQTEQ-PB_v10_WEB.pdf)
- [19] Y. M. Ramos, R. M. Arias, J. A. Bosch, R. A. Estrada, «Análisis Numérico Comparativo del Comportamiento a Fatiga de osteosíntesis utilizadas en el tratamiento de la fractura de cadera 31 A1. 1.» [https://www.scielo.org.mx/scielo.php?script=sci\\_arttext&pid=S1405-77432017000400445](https://www.scielo.org.mx/scielo.php?script=sci_arttext&pid=S1405-77432017000400445)
- [20] J. Jiménez M, «Large Bone Fracture, Tables and Figures – Long Bone Fracture.pdf», [https://github.com/jjm20766/Large\\_Bone\\_Fracture](https://github.com/jjm20766/Large_Bone_Fracture)